Journal of Applied Physics

Metal–organic frameworks under pressure

Cite as: J. Appl. Phys. **126**, 181101 (2019); https://doi.org/10.1063/1.5126911
Submitted: 06 September 2019 • Accepted: 21 October 2019 • Published Online: 11 November 2019

Ines E. Collings and Andrew L. Goodwin

Journal of Applied Physics TUTORIAL scitation.org/journal/jap

Metal–organic frameworks under pressure

Cite as: J. Appl. Phys. **126**, 181101 (2019); doi: 10.1063/1.5126911
Submitted: 6 September 2019 · Accepted: 21 October 2019 ·
Published Online: 11 November 2019

Ines E. Collings[1] and Andrew L. Goodwin[2,a)]

AFFILIATIONS

[1]Center for X-ray Analytics, Swiss Federal Laboratories for Materials Science and Technology, Überlandstrasse 129, 8600 Dübendorf, Switzerland
[2]Department of Chemistry, Inorganic Chemistry Laboratory, University of Oxford, South Parks Road, Oxford OX1 3QR, United Kingdom

[a)]andrew.goodwin@chem.ox.ac.uk

ABSTRACT

Metal–organic frameworks (MOFs) are a broad and interesting class of materials known for their mechanical flexibility. As such, their response to pressure is usually extreme and often counterintuitive. This tutorial review surveys the structural response of MOFs to pressure as observed experimentally. It describes the experimental tools exploited in high-pressure crystallographic measurements and highlights some of the experiment design choices that influence the actual physics probed in these measurements. The main focus of the review is a description of the key pressure-driven structural responses exhibited by MOFs: isosymmetric compression, including negative compressibility; symmetry-lowering transitions; changes in connectivity; amorphization; and inclusion of the pressure-transmitting medium within the MOF pores. The review concludes both by highlighting some functional implications of these responses and by flagging some future directions for the field.

I. INTRODUCTION

Metal–organic frameworks (MOFs) are a class of materials comprising inorganic nodes—such as transition-metal cations or polyoxometallate clusters—and organic linkers.[1,2] The linkers connect the nodes to form extended network structures of varying topologies, such as those of the few canonical examples shown in Fig. 1(a). The use of "molecular" linkers in MOFs not only gives rise to a huge chemical diversity, but also to structures that are intrinsically and profoundly flexible.[3,4] This flexibility is activated readily in response to most external stimuli, such as changes in temperature or pressure and/or guest adsorption.[5,6] Here, we are particularly concerned with the pressure-driven responses of MOFs. Our motivation derives from the observation that the particular flexibility of MOFs translates to extreme—and often very useful—physical behavior.

Pressure is one of the most revealing thermodynamic variables used in studying materials, since it is now experimentally possible to access pressures that are four to six orders of magnitude greater than ambient conditions (i.e., 1–100 GPa).[7] The thermodynamic implications of this high-pressure regime are all the more important for "soft" materials, such as MOFs. In this context, it is hardly surprising that MOFs show a wide variety of physical responses to pressure—even at the relatively modest 1 GPa level. Moreover, because it is possible to measure X-ray diffraction patterns at these pressures, we now have an increasingly detailed microscopic understanding of the structural changes that take place in MOFs under these elevated pressures.

In this tutorial review, we survey the main structural mechanisms by which MOFs respond to pressure [Fig. 1(b)], as observed experimentally. We are by no means the first to attempt such a survey,[5,8–10] and we note, in particular, the excellent (and more in-depth) review given on this specific topic in Ref. 9. We would also highlight the computational and theoretical perspectives developed in Ref. 11. Here, we have tried to focus mostly on some key developments in the literature since those reviews, but many of the core principles are of course entirely in common. Our own starting point is a description of the experimental tools available for high-pressure crystallographic measurements, together with some of the important considerations that can affect the physics actually probed by these measurements. In Sec. III, we develop each of the response mechanisms depicted graphically in Fig. 1(b), drawing on examples from the recent literature. What follows in Sec. IV is a summary of the various pressure-driven "functional" responses of MOFs, including piezochromism, magnetism, spin crossover, and barocaloric

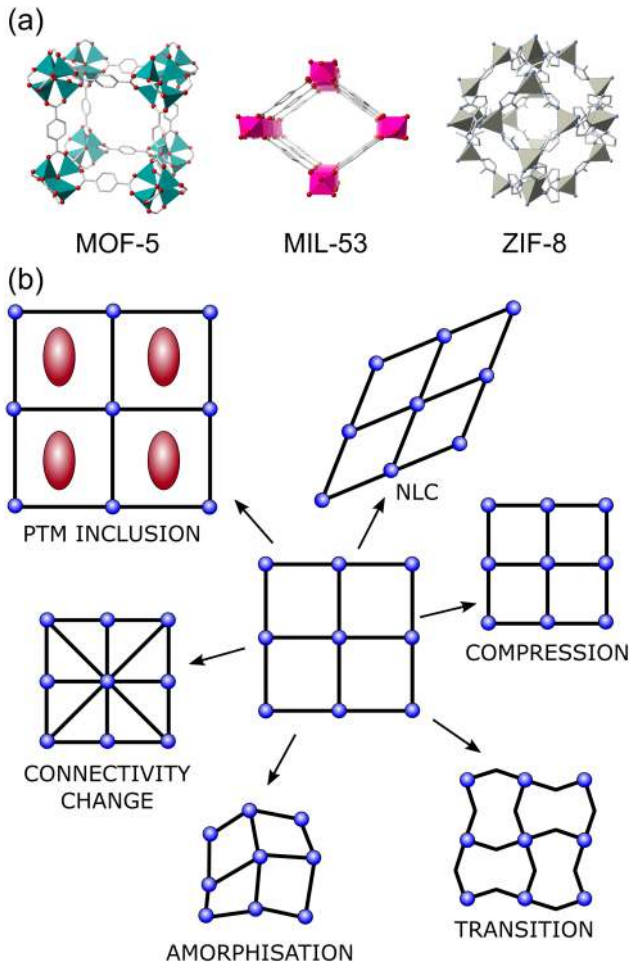

FIG. 1. (a) Representations of the structures of some canonical MOFs, highlighting their porous nature. In each case, metal coordination environments are shown as filled polyhedra, and organic linkers are shown in stick representation. The chemical formulas for MOF-5, MIL-53, and ZIF-8 are $Zn_4O(bdc)_3$, where bdc = benzene-1,4-dicarboxylic acid, $M^{III}(OH)(bdc)$, and $Zn(mim)_2$, where mim = 2-methylimidazolate, respectively. (b) Schematic representation of the various pressure-induced responses most frequently exhibited by MOFs.

behavior. Our aim is to demonstrate how pressure might be used rationally to control the physical properties of MOFs via interplay with the underlying structure. The review concludes with a perspective for some future direction of high-pressure studies of MOFs: where might the field head?

Before embarking, we make one observation that links what we are about to cover with the more widely studied phenomenology of guest adsorption/desorption in MOFs. When synthesized, porous MOFs almost invariably contain solvent molecules within their pores. Hence, the framework is effectively under negative (internal) pressure, such that the process of solvent removal is conceptually related to the application of external pressure. It is no accident that the various structural responses outlined here share much in common with those activated under guest release.[5] Consequently, an understanding of the high-pressure behavior of MOFs can provide important insight into ambient-pressure guest-dependent behavior, which in turn is important for many of the famous applications of MOFs: gas storage, molecular separation, chemical sensing, and drug delivery.

II. EXPERIMENTAL SETUP FOR HIGH PRESSURE

This section aims to give a brief overview of the key considerations for high-pressure experimental studies of MOFs, focusing on those experimental methods used to investigate MOFs so far. Many excellent reviews describe the history, preparation, and measurement procedures of high-pressure diffraction experiments in much more detail, such as those given in, e.g., Refs. 12–15.

A. High-pressure cells

A diamond-anvil cell (DAC) is the most readily available and versatile apparatus for the application of pressure [Fig. 2(a)]. Briefly, it consists of two metal parts that each hold the assembly of a supporting seat with an opening at the center for the positioning of a diamond anvil. The pressure is generated by opposing anvils, as was first designed by Bridgman.[16] Diamonds are ideal for the generation of high pressures and are also transparent to a range of different electromagnetic radiation, thus facilitating *in situ* high pressure measurements. Many different body designs exist to hold together the assembly of anvils; for example, the Merrill-Bassett,[17] LeToullec,[18] and BX90[19] designs [Figs. 2(a) and 2(b)]. Both body parts fit together to allow a perfect alignment of the culets from the diamonds. A drilled indented gasket sits in between the two diamond culets and forms a pressure chamber for the sample, pressure-transmitting medium (PTM), and ruby spheres or quartz for pressure calibration [Fig. 2(c)]. Typically, the gasket is a metal sheet of stainless steel, tungsten, or rhenium (to achieve higher pressure). The presence of PTM allows the stress generated through uniaxial compression to be evenly distributed over the sample, with the aim of generating hydrostatic conditions. The thickness of the sample should also be taken into account in order to avoid bridging between the diamond anvils up to the maximum pressure to be studied. The anvils are brought closer together by either mechanical force—such as the tightening of screws connecting the two body parts—or through a pneumatic driving mechanism by altering the gas pressure on a membrane acting on the diamond assembly. The pressure in the gasket chamber is usually determined by measuring the shift in the R1 line from the ruby fluorescence[20,21] or via the change in the unit cell of a calibrant such as quartz.[22]

B. Pressure-transmitting medium

As discussed above, a PTM should be included within the sample chamber to ensure hydrostatic conditions on the sample. There is a large choice of different PTMs, ranging from oils or alcohol mixtures to gases.[24] However, special consideration of the PTM is needed in the case of MOFs, since they are intrinsically porous materials that can allow entry of the PTM within the MOF pores. The compression of MOF·PTM often leads to a different pressure-dependent behavior when compared to the MOF

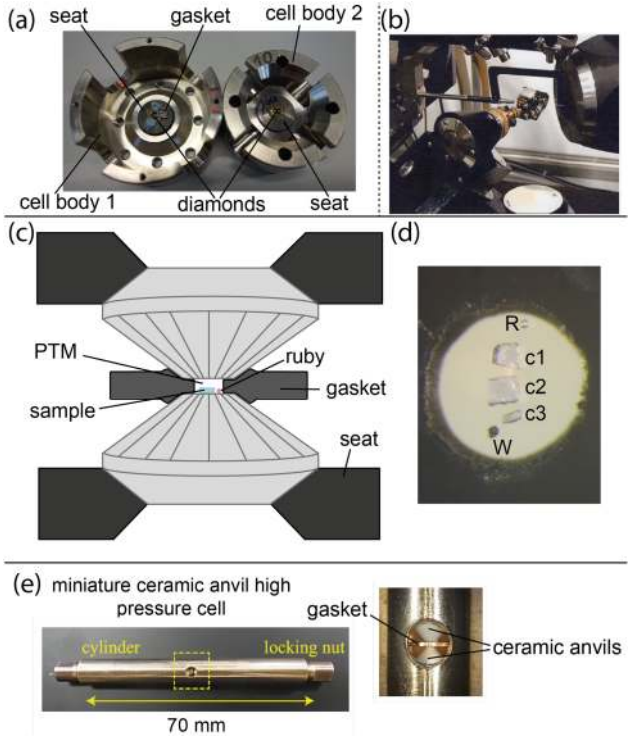

FIG. 2. (a) Example of a DAC with the two metal body parts shown. Inside each metal part is the assembly of a seat with a diamond glued in the middle. The gasket is also shown offset to its usual position on top of one of the diamonds. (b) Example of a Merrill-Bassett DAC in position on a X-ray diffractometer. Reproduced with permission from Katrusiak, Acta Crystallogr. A **64**, 135 (2008). Copyright 2008 International Union of Crystallography. (c) Schematic of the diamond-anvil assembly with the Boehler-Almax design of the diamonds. (d) Example of a single-crystal loading for synchrotron X-ray diffraction with the positioning of a ruby (R), three single crystals (c1,c2,c3), and a piece of tungsten (W) for centering purposes. (e) Example of a miniature ceramic anvil high pressure cell used for magnetic measurements. Adapted from Tateiwa *et al.*, J. Phys. Conf. Ser. **500**, 142032 (2014). Copyright 2014 Author(s), licensed under a Creative Commons Attribution 3.0 Unported License.[23]

compressed in a nonpenetrating PTM, as will be discussed in more detail in Sec. III E. In addition, MOFs also have a propensity for reacting with or dissolving in the PTMs (especially in the case of alcohol-containing mixtures).[25] We note that this route may lead to the high-pressure synthesis of new MOF structures *in situ*.[26] The choice of PTM also affects the pressure range over which hydrostatic conditions might be expected, due to the different solidification pressures for different PTMs.[24,27] We note that MOFs may be particularly sensitive to a change in hydrostaticity due to their more flexible and responsive nature.

C. Types of high-pressure measurements

The mode of compression and any pressure-dependent physical properties of a sample can be studied within a diamond-anvil cell using a variety of different measurements. The most common such measurement involves structural studies via X-ray diffraction, using powder and/or single crystal measurements. In this way, it is possible to determine the effect of pressure on both unit cell and atomic-scale structure (mainly determined from single-crystal data). Infrared (IR) and Raman spectroscopic measurements also offer important insight into the pressure dependence of the vibrational modes that arise from bonded interactions in the structure. Such measurements can also be used to study noncrystalline samples under pressure. For physical property measurements under pressure, such as magnetic measurements,[28–31] the standard diamond-anvil cell design needs to be adapted in order to fit the confinement of a superconducting quantum interference device (SQUID) magnetometer [Fig. 2(e)].

The use of neutron diffraction to study the high-pressure structural behavior of MOFs is much less common. This is understandable enough, given the requisite access to central facilities, the limitation to powder diffraction—although developments in high-pressure single-crystal diffraction are advancing[32]—and the complications and cost of deuteration. Usually, large-volume presses, such as the Paris-Edinburgh press,[33] or clamp cells[34] are used for neutron high-pressure powder diffraction experiments because the weak scattering by neutrons necessitates larger sample volumes. In such cases, a calibrant (often Pb) is added to the sample chamber in order to determine the pressure from the corresponding lattice parameter variation.[35]

D. Structural studies under pressure

Powder diffraction measurements are the most straightforward means for determining compressibility and phase behavior of a MOF sample under pressure. However, the structure solution of any new high-pressure phases observed or determination of atomic-scale structural changes under pressure often require either the aid of computational modeling[36–38] or the use of single-crystal diffraction experiments. This is especially true for MOFs, given their relatively complex crystal structures.

Three main technical aspects (not relating to the sample quality) help optimize the quality of X-ray diffraction data and hence improve the chances of determining compression mechanisms. These are (i) a large DAC opening angle, (ii) a highly parallel and small X-ray beam, and (iii) collection with a large, sensitive 2D area detector. The opening angle of a DAC dictates the diffraction cone available for the measurement; the greater the opening, the higher the resolution of the diffracted data. The X-ray wavelength and sample-to-detector distance can also be optimized to ensure measurements to high resolution. In the case of single-crystal data, the opening angle of the DAC also regulates the fraction of reciprocal space that can be explored, which is especially important for low-symmetry crystals. One design strategy that has been implemented to ensure a wide opening angle (~85°) is to use Boehler-Almax diamonds,[39] coupled with suitably large seat and body cell openings [Fig. 2(c)].

III. STRUCTURAL CHANGES UNDER PRESSURE

Having established the experimental requirements for measuring the pressure-dependent structural behavior of MOFs, we turn now to the various possible types of behavior one might observe.

Our starting point is to consider straightforward compressibility mechanisms, where there is no fundamental change in MOF symmetry or topology. Such mechanisms usually dominate the low-pressure behavior of MOFs. At higher pressures, it is typical for the system to exhibit a phase transition. This might be displacive so that the MOF topology is conserved or reconstructive. Arguably, the most complex situation (albeit a relatively common one for MOFs) is the loss of crystallinity altogether, via pressure-induced amorphization. Finally, we consider the possibility of interaction between a MOF and the pressure-transmitting medium used in compression measurements. These interactions can lead to ostensibly spurious behavior, such as an apparent negative volume compressibility.

A. Compression mechanisms: Isotropic and anisotropic

The simplest compression response of a MOF—as for any other material—is isotropic compression in all three crystallographic directions. This is certainly the fundamental response of a cubic system (in the absence of any guest inclusion). In such cases, the pressure response depends solely on how effectively the M–ligand–M units can contract. The flexibility in the ligand,[40–42] its functionalization,[43–46] length,[42] and aromaticity, as well as the degree of porosity,[42] will have an impact on the MOF's resistance to pressure. This resistance is captured by the bulk modulus

$$B_0 = -V\left(\frac{\partial p}{\partial V}\right)_T, \tag{1}$$

which reflects the pressure required to produce a given relative change in volume. The larger the value of B_0, the stiffer the material. For conventional ceramics, $B_0 \simeq 10$–100 GPa; the corresponding values for MOFs are usually about one order of magnitude lower.[47] The value of B_0 is determined experimentally from the pressure dependence of the MOF unit cell volume by fitting to a suitable equation of state.[48–50]

Both experimental and computational studies have explored methods of enhancing the mechanical stability of MOFs. A recent high-throughput computational study correlated bulk modulus with framework topology, linker length, and coordination number.[51] More specific computational studies have found that strategic functionalization of linkers can help maintain mechanical stability by increasing the connectivity via nonbonded interactions or by changing the electron-withdrawing power of the linker.[45,46] For example, zeolitic imiadazolate frameworks (ZIFs) with bulky functional groups have been shown to be more resilient to pressure than those with less bulky substituents.[52,53] Likewise, MOF frameworks can in general be made more rigid by increasing their connectivity, which in turn improves mechanical stability.[54,55]

A topic of some considerable currency is the effect of defects on the compressibility of MOFs. Settling this point is challenging because defect structures may change from sample to sample, and varying degrees of solvation/hydration on the defect sites may also give rise to differences in compressibility. For example, a study of defective UiO-66 $[Zr_6O_4(OH)_4(bdc)_6]$ found that the bulk modulus first decreases up to a certain critical defect concentration.[56] Beyond this critical defect level, the bulk modulus did not change significantly with increasing defect concentrations. It is thought that this behavior may be related to the distribution and type of defects in the structure: a computational study on UiO-66 showed that defect arrangements could affect the value of the bulk modulus by as much as 4.4 GPa.[57]

For anisotropic (noncubic) MOFs, there is no requirement that the crystal structure compresses by equal rates in different directions. By fitting the pressure dependencies of the lattice parameters, it is possible to determine the principal components of the compressibility tensor, and the relative differences among these three values reflect the extent of mechanical anisotropy.[49] Such anisotropy is usually a consequence of geometric (but not topological) changes to the MOF architecture (Fig. 3). By this, we mean that compression changes linker–node–linker angles far more than it does node–linker–node distances: the framework "hinges." When these geometric mechanisms dominate over conventional bond compression, then negative linear compressibility (NLC) can occur.[58–64] In favorable cases, the expansion from hinging and the bond contraction can almost exactly cancel out. This results in near-zero compressibility along one or two axes, as has been observed in guanidinium cadmium formate.[65] The rate of bond compression and framework hinging may change upon compression, giving rise to transitions between NLC and positive linear compressibility (PLC) along certain axes at some critical pressure value.[66,67] These transitions can proceed in either direction: NLC to PLC or vice versa. Other mechanisms for NLC have been proposed; for example, the torsional flexibility of polyhedra[68] and sliding of layers in 2D MOFs.[69]

The expansion of two directions under pressure, known as negative area compressibility (NAC), is much rarer than NLC but has nevertheless been observed in a few MOFs and related systems.[70,71]

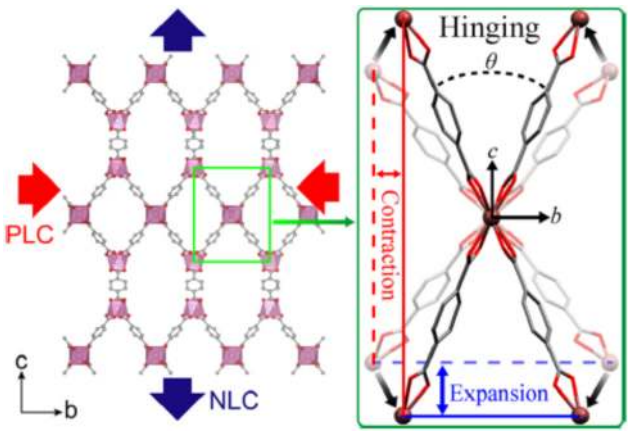

FIG. 3. Anisotropic compression in $InH(bdc)_2$ involves framework hinging. In turn, this gives a positive linear compressibility (PLC) response in one set of directions (red arrows), which couples to negative linear compressibility (NLC) in a perpendicular direction (blue arrows). Reprinted with permission from Zeng *et al.*, J. Am. Chem. Soc. **139**, 15648 (2017). Copyright 2017 American Chemical Society.

The dominant mechanism involves flattening of 2D layers within the MOF (e.g., puckered rings). The concomitant expansion within the layer directions is accompanied by a reduction in the spacing between these layers. Hence, the system expands in two directions and contracts in one. Both NLC and NAC are of interest in the development of artificial muscles, sensors, and actuators.[59]

In terms of the underlying physics, NLC and NAC arise from the presence of large and negative off-diagonal terms $S_{i\neq j}$ in the compliance tensor—i.e., the inverse of the elastic tensor. As a consequence, the existence of NLC or NAC is usually diagnostic of a range of anomalous mechanical properties, including negative thermal expansion and extreme Poisson anisotropy.[5,59,72]

B. Displacive phase transitions

Once the various bond and angle distortions allowed by symmetry have reached their physical limit during compression of an ambient-pressure MOF phase, a displacive transition that lowers symmetry may activate in order to allow additional distortion mechanisms. In most cases, a reduction in pore volume is the driving force for such pressure-induced phase transitions.

The structural complexity of MOFs and the propensity for high-pressure phase transitions to reduce crystallinity mean that the structures of only a few high-pressure MOF phases have been solved to date. Exploiting *ab initio* calculations and the relationship between high-pressure and (known) low-temperature structures collectively help to resolve potential high-pressure phases, especially when determined from powder diffraction data.

Using such approaches, we know, for example, that a reasonably common type of pressure-induced phase transition is that from so-called open-pore (op) to closed-pore (cp) states [Fig. 4(a)]; such transitions have been studied in at least two main classes of MOFs. One of the largest volume changes observed is for evacuated MIL-type frameworks,[36,37,73–75] where the op–cp transitions can allow up to 43% contraction, e.g., for MIL-47 [$V^{IV}O$(bdc)]. In this particular case, the transition is at just ∼0.2 GPa, which reflects the low energy barrier to phase interconversion.[36] This same type of transition is also observed for the evacuated zeolitic imidazolate frameworks ZIF-4 [$Co(im)_2$ and $Zn(im)_2$, im = imidazolate], which exhibit a 20% volume change at even lower pressures of 0.03–0.05 GPa.[76,77]

Variation of the nature of the metal cation from which these MOFs are assembled can change the onset pressure of the op–cp transition, while the reversibility can depend on the maximum pressure reached during compression.[76,77] Indeed, it is not always clear that the experimental behavior observed in compression experiments is equilibrium in nature or whether kinetic trapping is important. For example, the behavior of ZIF-4 upon rapid compression (2.5 GPa min^{-1}) was recently investigated, and the system was found to exhibit an altogether different phase behavior: two previously-unknown phases formed during compression, before amorphization at much higher pressures of 7 GPa[53] (cf. 1–2 GPa in Ref. 76). Nonequilibrium behavior during rapid compression, the effects of radiation damage, and the role of included/excluded solvent may account for this difference in behavior.[79]

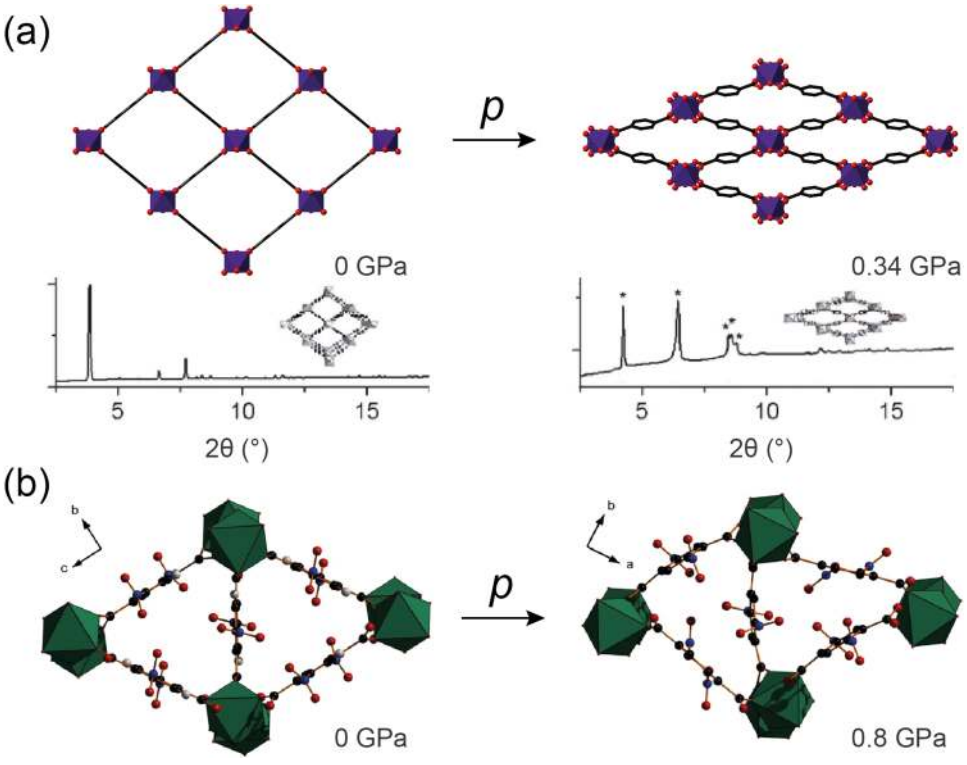

FIG. 4. Displacive transitions upon compression in (a) MIL-47(V^{VI}) arising from an op-cp change with the corresponding powder diffractions shown[36] and (b) $Sc_2(NO_2-bdc)_3$ from octahedral rotations.[78] Panel (a) is adapted with permission from Yot *et al.*, Chem. Sci. **3**, 1100 (2012). Copyright 2012 The Royal Society of Chemistry. Panel (b) is adapted with permission from Graham *et al.*, J. Am. Chem. Soc. **136**, 8606 (2014). Copyright 2014 American Chemical Society.

Denser MOFs—e.g., those with minimal pore volume, those containing included guests, or those with interpenetrated frameworks—also show displacive phase transitions under pressure, but the change in volume is usually much less than for the porous MOFs described above (of the order of $\Delta V/V \simeq 2$–5%).[44,61,80–84] Especially when the pore volume is limited, a reduction in volume is often accommodated by tilting of the metal coordination polyhedra [Fig. 4(b)][78,80,85–87] and/or changes in the binding geometry of the metal–ligand–metal linkages.[26,80,81,85] The former mechanism is closely related to compression mechanisms in conventional ceramics (i.e., activation of octahedral tilts), but the latter mechanism is unique to molecular frameworks. The degree of structural flexibility exhibited by a given MOF is often linked to the metal cation size (or, more precisely, its charge density), which in turn correlates inversely to the onset pressure of symmetry-breaking phase transitions.[44,80,88]

In dense MOFs containing molecular guest species, including extra-framework cations, the activation of symmetry-lowering framework distortions can couple to quenching of orientational degrees of freedom of the guest. This mechanism can induce orientational disorder–order transitions, such as observed for the dimethylammonium metal formates.[80] The associated changes in molecular degrees of freedom and lowering of symmetry at the guest site can be deduced both from crystallographic measurements and using high-pressure Raman spectroscopy.[89–92]

Correlated polyhedral tilts are by no means the only volume-reducing distortion mechanism accessible to MOFs. For brevity, we flag just one other example: namely, that the pressure-driven phase transition in $Co_2(bdc)_2dabco \cdot H_2O$ involves a change in ligand orientation.[93]

C. Reconstructive phase transitions

Reconstructive high-pressure phase transitions, where there is no requirement for a group/subgroup relationship between low- and high-pressure forms, can occur upon bond breakage and/or bond formation, usually within the metal coordination sphere. Such transitions often arise due to changes in ligand orientation and position upon compression and/or as part of a densification process characterized by an increase in framework connectivity.

The latter process appears to be especially important for small ligands, where a change in bonding state can be achieved relatively straightforwardly. For example, in metal formate frameworks of the composition $[tmenH_2][M(HCOO)_4]_2$ (here, $tmenH_2^{2+}$ = *N*, *N*, *N*′,*N*′-tetra-methylethylenediammonium and $M = Er^{3+}$ or Y^{3+}), the connectivity of the framework topology increases on compression as some formate linkers switch from binding only a single rare-earth ion (chelating mode) to binding a pair of ions (bridging mode) (Fig. 5).[94,95] The coordination number of the M^{3+} ion is unchanged in the process. A similar mechanism operates in $CoCl_2bpp$ [bpp = 1,3-bis(4-pyridyl)propane], as Cl^- ligands switch to bridging Co centers in the high-pressure phase.[96] However, in this case, there is an increase in the coordination number from four to six at the Co site. A change in color accompanies this change in coordination number, and so this particular dense MOF is piezochromic.[96] We discuss this point in more detail below.

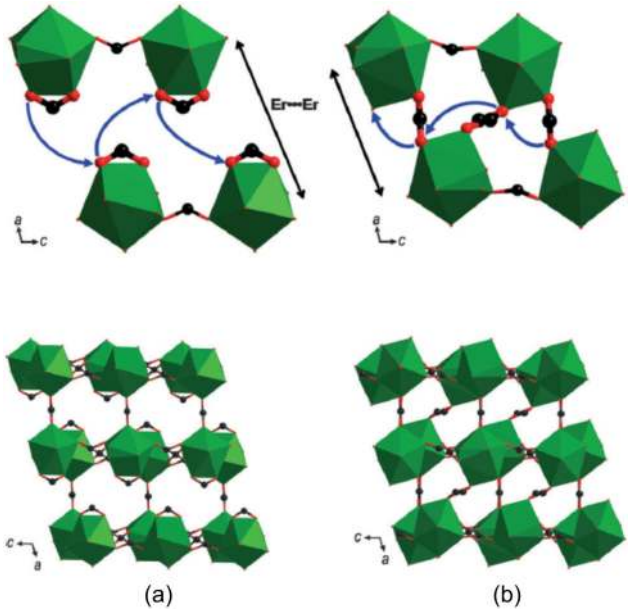

FIG. 5. Bond rearrangement in $[tmenH_2][Er(HCOO)_4]_2$, increasing the connectivity of the framework from the (a) ambient-pressure to (b) high-pressure phase. Er coordination polyhedra are shown in green. Reprinted with permission from Spencer *et al.*, Angew. Chem. Int. Ed. **53**, 5583 (2014). Copyright 2014 John Wiley and Sons.

High pressures can cause changes in metal coordination numbers by favoring the binding of otherwise unbound donor atoms. In $Zn(GlyTyr)_2$ (GlyTyr = glycyl-L-tyrosine), for example, there is a pressure-induced phase transition at 2 GPa that involves binding of additional oxygen donors of the amino acid carboxylate groups at the Zn^{2+} site.[40] The cation coordination geometry changes from tetrahedral to octahedral in this process. The additional donor need not come from the MOF linkers and can instead involve coordination of included guest molecules,[97] such as in the compound $[Co_3(OH)_2btca_2] \cdot 2DMF$ (btca = benzotriazolide-5-carboxylate; DMF = *N*,*N*-dimethylformamide). In this case, the Co^{II} centers change coordination number from five to six upon compression as DMF is coordinated.[98]

One of the few cases of bond rearrangement in a MOF under pressure that occurs without change to the coordination number of the metal center was observed for the dense zinc imidazolate with "zni" topology [often known as ZIF-zni, with the formula $Zn(im)_2$].[99] Remarkably, this high-pressure phase could be recovered back to ambient conditions, allowing its structure to be solved and refined *ex situ*.

In all the examples given above, pressure favors bond rearrangements that increase connectivity and/or metal coordination numbers. Rather counterintuitively, there is an example of a bond rearrangement mechanism that reduces the connectivity from a 1D coordination polymer to a discrete dinuclear complex: namely, for $[Cu_2L_2(1-methylpiperazine)_2]_n$, where H_2L is 1, 1′-(1,3-phenylene)-bis(4,4-dimethylpentane-1,3-dione).[100] In this case, it is

the increased packing efficiency of the Cu_2L_2 units that appears to drive bonding rearrangement.

For MOFs containing hydrogen-bonded molecular cations in the framework pores—e.g., in the protonated amine metal formates—pressure can change the hydrogen bonding network of the protonated amines. This has been observed for the high-pressure transition of guanidinium metal formates $[C(NH_2)_3]M(HCOO)_3$ ($M = Mn^{2+}$, Co^{2+}). Their structures transform under pressure from *Pnna* to $R\bar{3}c$ symmetries, with the transition involving a change in the packing of the guanidinium cation and thus of the hydrogen bonding network.[101,102]

D. Pressure-induced amorphization

Amorphization can be considered an extreme case of symmetry lowering, in which no symmetry elements are preserved. In conventional ceramics, pressure-induced amorphization (PIA) is sometimes framed in the context of multi-**q** transitions.[103] For sufficiently flexible materials, pressure-induced mode softening occurs simultaneously across many branches of the phonon dispersion, leading to a transition characterized by a broad spectrum of wavevectors. Given the mechanical softness of MOFs[47] and their propensity to support many branches of low-energy phonon modes spread throughout the Brillouin zone,[104] it is perhaps unsurprising that PIA is not at all rare among MOFs.

Probably, the first well-characterized example of PIA in a MOF was that of ZIF-8 (Fig. 6).[105] Under ambient conditions, ZIF-8 has the sodalite topology, so its amorphization is conceptually related to that of zeolites.[106] As for zeolites, the transformation is irreversible, and the recovered *a*-ZIF-8 is not porous. Other MOFs—such as ZIF-4, ZIF-7 [$Zn(bim)_2$ where bim = benzimidazolate], and ZIF-62 [$Zn(im)_{1.75}(bim)_{0.25}$]—exhibit reversible amorphization.[52,107,108] This suggests that the transition is essentially displacive but activated across many **q**-vectors simultaneously (the ZIF-8 process is presumably reconstructive). For many other MOFs, pressure gives rise to a decrease in crystallinity, but with the retention of broad diffraction peaks.[76] This suggests partial amorphization. In these cases, one would expect that decompression back to ambient would restore the original crystallinity of the MOF, as the exhibition of diffraction peaks suggests that the connectivity is preserved. Factors such as radiation damage,[79,86] or compression of the MOF beyond the hydrostatic regime of the PTM may explain why decompression does not always restore crystallinity fully.

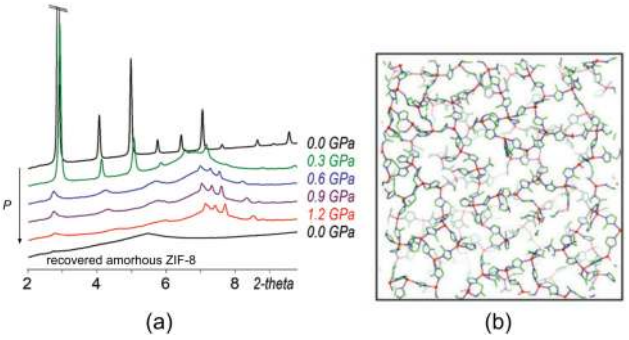

FIG. 6. Irreversible amorphization of ZIF-8. (a) Variable-pressure X-ray powder diffraction patterns, showing the loss of Bragg diffraction on compression and the irreversibility of the PIA process. Adapted with permission from Chapman *et al.*, J. Am. Chem. Soc. **131**, 17546 (2009). Copyright 2009 American Chemical Society. (b) Representation of a reverse Monte Carlo atomistic model developed in Ref. 109 to account for the X-ray scattering measured from an amorphized ZIF-8 sample generated using ball-milling. The configuration is itself based on that used to describe thermal amorphization in ZIF-4.[110] Adapted with permission from Cao *et al.*, Chem. Commun. **48**, 7805 (2012). Copyright 2012 The Royal Society of Chemistry.

Naively, one might expect that design approaches for stabilizing MOFs against amorphization should be essentially the same as those for maximizing B_0. However, it appears that—at least in some cases—increasing the flexibility of the linker used in a MOF can allow the system to retain crystallinity to higher pressures. This is seen explicitly in the case of the two MOFs UiO-67 [$Zr_6O_4(OH)_4(bpdc)_6$ where bpdc = 4, 4′-biphenyl dicarboxylate] and UiO-abdc [$Zr_6O_4(OH)_4(abdc)_6$ where abdc = 4, 4′-azobenzene dicarboxylate]. These two systems have the same "fcu" topology and very similar chemistries: they consist of zirconium-based clusters connected by aromatic dicarboxylate linkers. The UiO-abdc MOF contains the more flexible azobenzene linker (abdc). As expected, this is the softer of the two frameworks ($B_0 = 15.2$ GPa vs 17.4 GPa for UiO-67). However, it is also the more resilient to amorphization: there is a factor-of-six difference in the onset pressure for PIA.[111] It is possible that the springlike nature of the abdc ligand allows for more efficient storage of mechanical energy—and hence resistance to plastic deformation—as noted for other framework materials containing similar microscopic motifs.[112]

E. Guest inclusion

In each of the deformation mechanisms considered so far, the chemical composition of the MOF is unchanged during compression. Of course, in a high-pressure experiment, a given MOF is surrounded by a dense fluid—the PTM—and it is not at all uncommon for this fluid to interact with the MOF at high pressures. Thermodynamics demands that the volume of the system as a whole must decrease as pressure increases, and it is often the case for MOFs that this can be achieved by incorporation of the PTM within the MOF.[113] Indeed, this process usually increases the MOF molar volume, leading to the ostensibly anomalous "negative compressibility" of the system. There is no thermodynamic trickery, of course, since the system volume (MOF + PTM) is itself smaller after inclusion. We note the conceptual parallel to the phenomenology of "negative gas adsorption" in DUT-49 [Cu_2(bbcdc) where bbcdc = 9, 9′-([1,1′-biphenyl]-4,4′-diyl)bis(9*H*-carbazole-3,6-dicarboxylate)].[114]

The inclusion of PTMs within a MOF structure affects not only the molar volume, but modifies its pressure dependence (i.e., B_0)[115,116] and also the existence and nature of any high-pressure phase transition behavior.[78,117] A very important insight into this compression behavior is given by the location of possible adsorption sites and structural changes to the MOF upon incorporation of the guest.[118,119] Using suitable high-pressure structural studies, one can better interpret possible discontinuities in adsorption

isotherms. For example, a high-pressure single-crystal diffraction and computational study on ZIF-8 compressed in penetrating O_2, N_2, Ar, and CH_4 media showed the location of the relevant adsorption sites, giving an in-depth understanding of the adsorption mechanism of each of these gases (Fig. 7).[120] With regard to understanding hydrocarbon separations, the pressure-induced insertion of small hydrocarbons (employed as PTMs) in Sc_2bdc_3 showed how pore geometries—and, in particular, linker rotation angles—responded to gas uptake.[121]

Because guest inclusion can significantly influence compressibility, it is possible that the bulk modulus determined in high-pressure diffraction experiments can depend critically on the particular PTM used. For example, if UiO-abdc (and UiO-67) are compressed using methanol as PTM, then the methanol is adsorbed and the MOF compressibility is nearly zero. By contrast, the use of a nonpenetrating oil as PTM allows the system to reduce its volume by about 10% during compression, since the MOF pore network remains vacant throughout.[111] To make matters more complicated, the interaction between MOF and PTM is sometimes more pathological than a simple adsorption process, and the framework topology itself can rearrange as the PTM enters. Probably, the most exciting example of this behavior is observed in $Zn(CN)_2$ (not strictly a MOF, but closely related nonetheless): its ambient nonporous twofold interpenetrated diamondoid topology structure rearranges on compression to give porous diamondoid, ionsdaleite, or pyrite topologies.[86] The particular change in topology observed depends on the PTM used and the compression conditions.

Pore composition changes can also be induced when a smaller molecule from the PTM replaces a larger molecule held within the MOF's pores. This was demonstrated during the compression of $V^{III}(OH)(bdc)\cdot tpa$ (tpa = terephthalic acid), known as MIL-47(V). In this case, the tpa in the framework pores was replaced with methanol or water when compressed in either MeOH:EtOH:H_2O or H_2O, respectively.[122] Interestingly, in the case of full MeOH exchange with tpa, this exchange was not reversed on pressure release. Consequently, the application of pressure acts as a form of postsynthetic modification in this case (more on this below). In a similar vein, the application of pressure with suitably small molecule PTMs (e.g., MeOH, EtOH, MeCN) was also able to drive exchange of the coordinated water molecules to the copper paddlewheels in STAM-1 $[Cu(C_{10}H_6O_6)(H_2O)\cdot 1.66H_2O]$.[123]

MOFs that already contain guests within their pores prior to compression, or that have a saturated uptake of guests upon continued compression, can give rise to guest expulsion to allow larger framework deformation mechanisms. The example reported in Ref. 124 involves a MOF for which some fraction amorphizes under pressure, in turn expelling its constituent guests into the remaining crystalline component. In turn, this mass transfer process leads to an apparent expansion of the crystalline MOF with pressure. A similar phenomenon has also been observed with coordination polymers containing ions within their pores, such as $[C(NH_2)_3]_2[Cu(CO_3)_2]$. For this system, on squeezing beyond a critical pressure, there is apparently a transfer of guanidinium cations from the windows of the copper carbonate cages into the center of the cages, which in turn expands.[125] Overall, the samples exhibit a reduction in volume, but as diffraction is only sensitive to the crystalline material, only the volume expansion is detected.

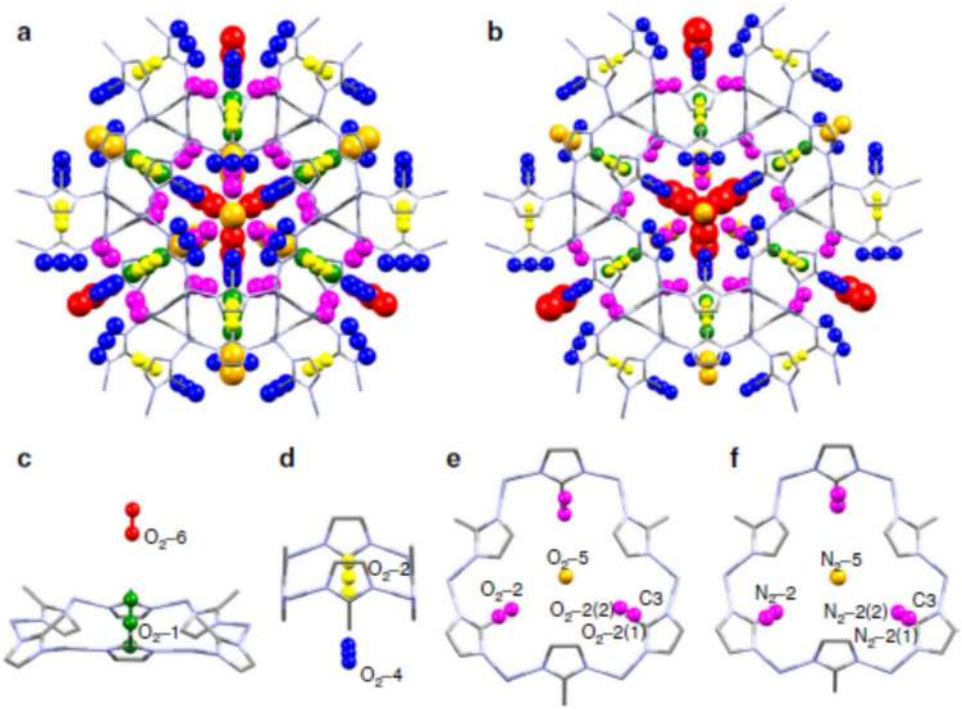

FIG. 7. Location of O_2 and N_2 binding sites within the pores of ZIF-8 at high pressure, determined using single-crystal diffraction measurements. Reproduced from Hobday *et al.*, Nat. Commun. **9**, 1429 (2018). Copyright 2018 Author(s), licensed under a Creative Commons Attribution 4.0 License.

IV. FUNCTIONAL RESPONSE TO PRESSURE

So far, we have surveyed the large number of different structural responses exhibited by MOFs at high pressures, together with the experiments one might carry out to determine these responses. From an applied physics perspective, however, high-pressure transformations in MOFs are of greatest importance if they affect physical properties. Pressure-driven property changes in MOFs can—and do—originate from variations in the molecular orbital energy levels, the configurational entropy of the system, charge distribution, orbital orientations, or magnetic exchange interactions. Here, we provide an extremely brief summary of some relevant examples.

Pressure-induced variations in transition-metal coordination geometries will affect the symmetry and energy of the *d*-orbitals via the crystal field. Consequently, for systems with suitable electronic configurations, one might expect pressure to influence color;[93,126] this is indeed the case for $CoCl_2$bpp, which shows a dramatic color change on compression (Fig. 8).[96] However, such piezochromism need not be confined to *d*–*d* transitions, and indeed pressure-dependent luminescence in lanthanide-based MOFs offers an interesting avenue for developing high-sensitivity pressure sensors.[127,128]

A quite remarkable effect of varying *d*-orbital energies under pressure occurs in the one-dimensional MOF $CuF_2(H_2O)_2(pyz)$ (pyz = pyrazine).[129] Under ambient conditions, the Cu^{2+} ion exhibits a strong first-order Jahn-Teller distortion—precisely as expected for a d^9 configuration in an octahedral crystal field. This distortion is manifested as a significantly greater Cu–N bond length, compared to the Cu–O and Cu–F bonds. In turn, this reflects the double occupation of a d_{z^2}-like orbital along the N–Cu–N axis. However, pressure switches the orientation of this doubly-occupied σ^* orbital: at ∼0.9 GPa, it lies along the O–Cu–O axis, and then from 3.1 GPa upwards, it lies along the F–Cu–F axis. Hence, pressure is tuning the orbital occupancies in this simple MOF.

A clear implication is that the magnetic exchange interactions should vary in each different regime. The importance of such variations has been shown most clearly in the closely-related material $[CuF_2(H_2O)_2]_2(pyz)$: here, pressure-driven orbital reorientation transitions take the system from a quasi-2D spin-$\frac{1}{2}$ square-lattice Heisenberg antiferromagnet to a system of weakly-coupled 1D Heisenberg chains.[130] Indeed, there are increasingly many reports of pressure-induced changes in magnetic behavior of coordination polymers.[81,131–134] Perhaps, the most striking report so far is the 50 K increase in long-range magnetic ordering temperature that occurs on compression to 4.7 GPa in the ferrimagnet $[Mn(en)]_3[Cr(CN)_6]_2 \cdot 4H_2O$ (en = ethylenediamine).[135]

Spin-state and charge localization transitions are also strongly sensitive to transition-metal *d*-orbital energies. So, it is no surprise that there are now a good number of pressure-induced high-spin/low-spin transitions known for Fe^{2+}-containing MOFs.[136–139] Charge transfer transitions are somewhat less widely studied, but we note the strong pressure-dependency of the charge transfer transition temperature $[Fe(2,2'\text{-bipyridine})(CN)_4]_2Co(4,4'\text{-bipyridine}) \cdot 4H_2O$: the rate of increase in T_c with pressure was found to be a remarkable 207 K kbar^{-1}.[140]

We discussed above the propensity for pressure to induce molecular orientation disorder/order transitions in dense MOFs. Such transitions are always associated with a substantial loss of configurational entropy, and this change in entropy allows such systems to be applied as barocalorics. The best studied system in this context is $[TPrA][Mn(dca)_3]$ (TPrA is tetrapropylammonium and dca is dicyanamide).[141] At ambient pressure, the material exhibits an order/disorder transition associated with reorientation of the $TPrA^+$ cation—this transition occurs at about $T_t \simeq 330$ K and is accompanied by an entropy loss/gain of 42.5 J kg^{-1} K^{-1}. Under hydrostatic pressure, the transition temperature increases (Fig. 9). Consequently, isothermal compression at temperatures just above T_t also drives a transition from the disordered to ordered states. The entropy change results in radiation of heat, such that on subsequent decompression, the system is forced to cool. Repeated compression/decompression cycles then form the basis for a strategy of solid-state refrigeration.

A final variation on this theme of using pressure to tune (favorably) the temperature at which structural transitions occur is

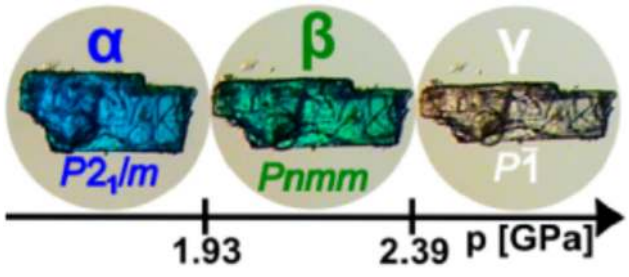

FIG. 8. Structural changes and increase in Co coordination of $CoCl_2$bpp under pressure leading to a piezochromic response. Adapted with permission from Andrzejewski and Katrusiak, J. Phys. Chem. Lett. **8**, 929 (2017). Copyright 2017 American Chemical Society.

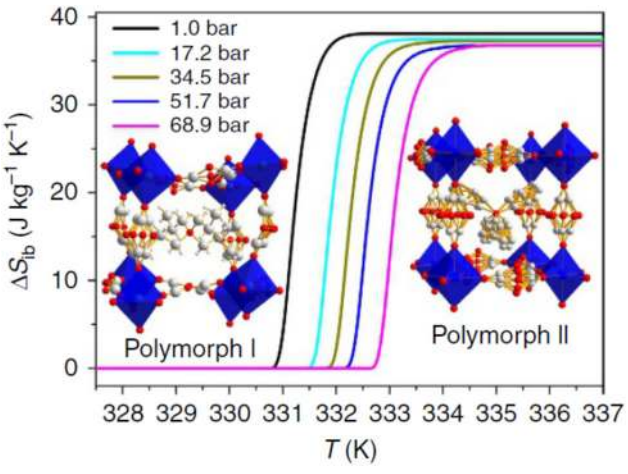

FIG. 9. Thermal entropy changes in $[TPrA][Mn(dca)_3]$ for a variety of applied pressures. Reproduced from Bermúdez-García *et al.*, Nat. Commun. **8**, 15715 (2017). Copyright 2017 Author(s), licensed under a Creative Commons Attribution 4.0 License.

that of pressure-induced melting in ZIFs. Liquid or glasslike MOFs are a potential source of entirely new types of functional optical materials, but are susceptible to chemical degradation during their thermal preparation.[142] It is now known that pressure can reduce the melting temperature of certain ZIFs, which in principle allows their synthesis at temperatures for which chemical degradation is less problematic.[108]

V. PERSPECTIVES AND OUTLOOK

In many ways, the use of high pressure to tune the functional responses of MOFs is a domain in its very infancy. Taking the various examples we have given here as a starting point, there is in nearly every case the potential to optimize the particular response of interest by varying MOF chemistry or topology. In this way, can we use pressure to drive magnetic ordering in MOFs to higher temperatures? Might we improve barocaloric figures of merit by using different organic cations to maximize entropy loss and reduce molar volume?

Looking beyond property optimization, one might reasonably seek inspiration from recent applications of high-pressure research in conventional ceramic materials. In that context, one particularly successful avenue of research has been the use of pressure to synthesize materials inaccessible under ambient conditions.[143] Some of the key lessons here have been that pressure can stabilize unusual valence states or metal coordination geometries. It would be a major coup for the MOF field if high-pressure synthesis opened up new chemistries that have typically been very difficult for the field to access: the incorporation of second- and/or third-row transition metal ions, for example, and/or the narrowing of HOMO/LUMO gaps to improve electronic conductivity. What is already known along these lines is that the compression of guest-containing MOFs can induce polymerization of the included components; an attractive example involves polymerization of iodine in a Ca (4,4′-sulfonyldibenzoate) MOF.[144] Indeed, we have already flagged one or two cases where high-pressure structural transformations appear irreversible on decompression—which in turn auger well for the applicability of high-pressure techniques as a MOF synthesis vector.

We have also seen that pressure can drive a variety of different symmetry-lowering transitions in MOFs, such as correlated tilts, collective Jahn-Teller order, and molecular orientational ordering. One of the conceptually appealing aspects of this diversity of phase transition behavior is the possibility of using a combination of suitable symmetry-lowering processes to drive the emergence of bulk polarization via a hybrid improper ferroelectricity mechanism.[145] It is now known that the various low-energy distortions accessible to MOFs are profoundly better suited to such an approach than are conventional ceramics.[146] So, for example, one might imagine using pressure to induce a set of correlated tilts or type of collective Jahn-Teller order that, when combined with orientational order of guest molecules, breaks inversion symmetry of the MOF.

From an experimental viewpoint, there are good reasons why the field has focused on hydrostatic compression of MOFs. However, given their propensity for unusual elastic behavior, there may be some significant mileage in exploring their response under uniaxial load. At face value, one expects anomalous Poisson behavior (both negative and extreme positive).[11,72,147] However, of course, the fundamental thermodynamic difference between hydrostatic and uniaxial conditions means that phase behavior may also be entirely different in this regime. In this context, we flag the potential application of MOFs in the absorption of mechanical energy—i.e., as shock absorbers.[148–150] There is the remarkable claim that some MOFs can absorb—gram for gram—as much energy as is released on detonation of 2,4,6-trinitrotoluene (TNT). Given that this nascent field has (understandably) focused on just one or two canonical MOF families, there is clear scope for understanding better mechanisms responsible for absorption of mechanical energy in general terms, in turn allowing for targeted material optimization.

On a much more fundamental level, our collective understanding of the soft-mode dynamics responsible for pressure-induced phase transitions in MOFs is conspicuously limited. The use of variable-pressure spectroscopic measurements in conjunction with the calculation of lattice dynamics from *ab initio* methods will be crucial in understanding the role and nature of phonon anharmonicity in MOF physics. We note that a number of MOFs are known to show negative thermal expansion,[151–153] and this important and interesting phenomenon is most fully understood through characterization of the pressure-dependencies of the phonon mode frequencies.[104,154] Indeed, given the relative small—if growing—number of fundamental studies of the response to pressure in different MOFs, we believe that there is enormous value in simply developing our empirical understanding by casting the MOF net wider—whether it be by studying a greater diversity of MOFs, by varying guest loading and type, by including and controlling vacancies, by varying composition, by studying magnetic or electronic or optical responses, or in any of various other ways we have tried to suggest in this review.

ACKNOWLEDGMENTS

A.L.G. gratefully acknowledges financial support from the European Research Council (Grant No. 788144) and many useful discussions with A. B. Cairns (Imperial), M. G. Tucker (Oak Ridge), N. P. Funnell (ISIS), and J. Haines (Montpellier). I.E.C. acknowledges the EMPAPOSTDOCS-II program that has received funding from the European Union's (EU) Horizon 2020 research and innovation program under the Marie Skłodowska-Curie Grant Agreement No. 754364.

REFERENCES

[1]O. M. Yaghi, M. O'keeffe, N. W. Ockwig, H. K. Chae, M. Eddaoudi, and J. Kim, Nature **423**, 705 (2003).
[2]G. Maurin, C. Serre, A. Cooper, and G. Férey, Chem. Soc. Rev. **46**, 3104 (2017).
[3]A. L. Goodwin, Phys. Rev. B **74**, 134302 (2006).
[4]L. Sarkisov, R. L. Martin, M. Haranczyk, and B. Smit, J. Am. Chem. Soc. **136**, 2228 (2014).
[5]F.-X. Coudert, Chem. Mater. **27**, 1905 (2015).
[6]A. Schneemann, V. Bon, I. Schwedler, I. Senkovska, S. Kaskel, and R. A. Fischer, Chem. Soc. Rev. **43**, 6062 (2014).
[7]W. A. Bassett, High Press. Res. **29**, 163 (2009).
[8]S. A. Moggach, A. J. Graham, A. Muszkiewicz, and C. A. Morrison, Int. J. Nanotechnol. **9**, 18 (2012).
[9]S. C. McKellar and S. A. Moggach, Acta Crystallogr. B **71**, 587 (2015).

[10]K. Yang, G. Zhou, and Q. Xu, RSC Adv. **6**, 37506 (2016).
[11]A. U. Ortiz, A. Boutin, A. H. Fuchs, and F.-X. Coudert, Phys. Rev. Lett. **109**, 195502 (2012).
[12]R. Miletich, D. R. Allan, and W. F. Kuhs, Rev. Mineral. Geochem. **41**, 445 (2000).
[13]A. Katrusiak, Acta Crystallogr. A **64**, 135 (2008).
[14]M. I. McMahon, *Advanced X-ray Crystallography*, Topics in Current Chemistry (Springer, Berlin, 2011), pp. 69–109.
[15]A. Katrusiak, *International Tables for Crystallography, Volume H, Powder Diffraction* (Wiley, Hoboken, NJ, 2019), pp. 156–173.
[16]P. M. Bridgman, *Nobel Lectures, Physics 1942–1962* (Elsevier, Amsterdam, 1946).
[17]L. Merrill and W. A. Bassett, Rev. Sci. Instrum. **45**, 290 (1974).
[18]R. Letoullec, J. P. Pinceaux, and P. Loubeyre, High Press. Res. **1**, 77 (1988).
[19]I. Kantor, V. Prakapenka, A. Kantor, P. Dera, A. Kurnosov, S. Sinogeikin, N. Dubrovinskaia, and L. Dubrovinsky, Rev. Sci. Instrum. **83**, 125102 (2012).
[20]R. A. Forman, G. J. Piermarini, J. D. Barnett, and S. Block, Science **176**, 284 (1972).
[21]J. D. Barnett, S. Block, and G. J. Piermarini, Rev. Sci. Instrum. **44**, 1 (1973).
[22]R. J. Angel, D. R. Allan, R. Miletich, and L. W. Finger, J. Appl. Crystallogr. **30**, 461 (1997).
[23]N. Tateiwa, Y. Haga, T. D. Matsuda, and Z. Fisk, J. Phys. Conf. Ser. **500**, 142032 (2014).
[24]S. Klotz, J.-C. Chervin, P. Munsch, and G. Le Marchand, J. Phys. D Appl. Phys. **42**, 075413 (2009).
[25]S. R. Madsen, S. A. Moggach, J. Overgaard, and B. Brummerstedt Iversen, Acta Crystallogr. B **72**, 389 (2016).
[26]S. Sobczak and A. Katrusiak, Inorg. Chem. **58**, 11773 (2019).
[27]R. J. Angel, M. Bujak, J. Zhao, G. D. Gatta, and S. D. Jacobsen, J. Appl. Crystallogr. **40**, 26 (2007).
[28]X. Wang and K. V. Kamenev, Low Temp. Phys. **40**, 735 (2014).
[29]Y. Feng, D. M. Silevitch, and T. F. Rosenbaum, Rev. Sci. Instrum. **85**, 033901 (2014).
[30]A. Marizy, B. Guigue, F. Occelli, B. Leridon, and P. Loubeyre, High Press. Res. **37**, 465 (2017).
[31]N. Tateiwa, Y. Haga, Z. Fisk, and Y. Ōnuki, Rev. Sci. Instrum. **82**, 053906 (2011).
[32]J. Binns, K. V. Kamenev, G. J. McIntyre, S. A. Moggach, and S. Parsons, IUCrJ **3**, 168 (2016).
[33]J. M. Besson, R. J. Nelmes, G. Hamel, J. S. Loveday, G. Weill, and S. Hull, Physica B **180–181**, 907 (1992).
[34]A. Podlesnyak, M. Loguillo, G. M. Rucker, B. Haberl, R. Boehler, G. Ehlers, L. L. Daemen, D. Armitage, M. D. Frontzek, and M. Lumsden, High Press. Res. **38**, 482 (2018).
[35]A. D. Fortes, I. G. Wood, M. Alfredsson, L. Vočadlo, K. S. Knight, W. G. Marshall, M. G. Tucker, and F. Fernandez-Alonso, High Press. Res. **27**, 201 (2007).
[36]P. G. Yot, Q. Ma, J. Haines, Q. Yang, A. Ghoufi, T. Devic, C. Serre, V. Dmitriev, G. Férey, C. Zhong, and G. Maurin, Chem. Sci. **3**, 1100 (2012).
[37]P. Ramaswamy, J. Wieme, E. Alvarez, L. Vanduyfhuys, J.-P. Itié, P. Fabry, V. Van Speybroeck, C. Serre, P. G. Yot, and G. Maurin, J. Mater. Chem. A **5**, 11047 (2017).
[38]M. Wahiduzzaman, N. Reimer, J.-P. Itié, N. Stock, G. Maurin, and P. G. Yot, Polyhedron **155**, 144 (2018).
[39]R. Boehler and K. De Hantsetters, High Press. Res. **24**, 391 (2004).
[40]J. Navarro-Sánchez, I. Mullor-Ruíz, C. Popescu, D. Santamaría-Pérez, A. Segura, D. Errandonea, J. González-Platas, and C. Martí-Gastaldo, Dalton Trans. **47**, 10654 (2018).
[41]K. J. Gagnon, C. M. Beavers, and A. Clearfield, J. Am. Chem. Soc. **135**, 1252 (2013).
[42]L. R. Redfern, L. Robison, M. C. Wasson, S. Goswami, J. Lyu, T. Islamoglu, K. W. Chapman, and O. K. Farha, J. Am. Chem. Soc. **141**, 4365 (2019).
[43]P. G. Yot, K. Yang, F. Ragon, V. Dmitriev, T. Devic, P. Horcajada, C. Serre, and G. Maurin, Dalton Trans. **45**, 4283 (2016).
[44]P. G. Yot, K. Yang, V. Guillerm, F. Ragon, V. Dmitriev, P. Parisiades, E. Elkaïm, T. Devic, P. Horcajada, C. Serre, N. Stock, J. P. S. Mowat, P. A. Wright, G. Férey, and G. Maurin, Eur. J. Inorg. Chem. **2016**, 4424.
[45]S. M. Moosavi, P. G. Boyd, L. Sarkisov, and B. Smit, ACS Cent. Sci. **4**, 832 (2018).
[46]B. Zheng, Y. Zhu, F. Fu, L. L. Wang, J. Wang, and H. Du, RSC Adv. **7**, 41499 (2017).
[47]J.-C. Tan and A. K. Cheetham, Chem. Soc. Rev. **40**, 1059 (2011).
[48]F. Birch, Phys. Rev. **71**, 809 (1947).
[49]M. J. Cliffe and A. L. Goodwin, J. Appl. Cryst. **45**, 1321 (2012).
[50]R. J. Angel, M. Alvaro, and J. Gonzalez-Platas, Z. Kristallogr. **229**, 405 (2014).
[51]P. Z. Moghadam, S. M. Rogge, A. Li, C.-M. Chow, J. Wieme, N. Moharrami, M. Aragones-Anglada, G. Conduit, D. A. Gomez-Gualdron, V. Van Speybroeck, and D. Fairen-Jimenez, Matter **1**, 219 (2019).
[52]P. Zhao, T. D. Bennett, N. P. M. Casati, G. I. Lampronti, S. A. Moggach, and S. A. T. Redfern, Dalton Trans. **44**, 4498 (2015).
[53]R. N. Widmer, G. I. Lampronti, S. Chibani, C. W. Wilson, S. Anzellini, S. Farsang, A. K. Kleppe, N. P. Casati, S. G. MacLeod, S. A. Redfern, F.-X. Coudert, and T. D. Bennett, J. Am. Chem. Soc. **141**, 9330 (2019).
[54]E. A. Kapustin, S. Lee, A. S. Alshammari, and O. M. Yaghi, ACS Cent. Sci. **3**, 662 (2017).
[55]A. U. Ortiz, A. Boutin, A. H. Fuchs, and F.-X. Coudert, J. Chem. Phys. **138**, 174703 (2013).
[56]S. Dissegna, P. Vervoorts, C. L. Hobday, T. Düren, D. Daisenberger, A. J. Smith, R. A. Fischer, and G. Kieslich, J. Am. Chem. Soc. **140**, 11581 (2018).
[57]S. M. J. Rogge, J. Wieme, L. Vanduyfhuys, S. Vandenbrande, G. Maurin, T. Verstraelen, M. Waroquier, and V. Van Speybroeck, Chem. Mater. **28**, 5721 (2016).
[58]A. B. Cairns, J. Catafesta, C. Levelut, J. Rouquette, A. van der Lee, L. Peters, A. L. Thompson, V. Dmitriev, J. Haines, and A. L. Goodwin, Nat. Mater. **12**, 212 (2013).
[59]A. B. Cairns and A. L. Goodwin, Phys. Chem. Chem. Phys. **17**, 20449 (2015).
[60]W. Li, M. R. Probert, M. Kosa, T. D. Bennett, A. Thirumurugan, R. P. Burwood, M. Parinello, J. A. K. Howard, and A. K. Cheetham, J. Am. Chem. Soc. **134**, 11940 (2012).
[61]W. Cai and A. Katrusiak, Nat. Commun. **5**, 4337 (2014).
[62]P. Serra-Crespo, A. Dikhtiarenko, E. Stavitski, J. Juan-Alcañiz, F. Kapteijn, F.-X. Coudert, and J. Gascon, CrystEngComm **17**, 276 (2015).
[63]Q. Zeng, K. Wang, and B. Zou, J. Am. Chem. Soc. **139**, 15648 (2017).
[64]Y. Yan, A. E. O'Connor, G. Kanthasamy, G. Atkinson, D. R. Allan, A. J. Blake, and M. Schröder, J. Am. Chem. Soc. **140**, 3952 (2018).
[65]Q. Zeng, K. Wang, and B. Zou, ACS Appl. Mater. Interfaces **10**, 23481 (2018).
[66]J. M. Ogborn, I. E. Collings, S. A. Moggach, A. L. Thompson, and A. L. Goodwin, Chem. Sci. **3**, 3011 (2012).
[67]H. H.-M. Yeung, R. Kilmurray, C. L. Hobday, S. C. McKellar, A. K. Cheetham, D. R. Allan, and S. A. Moggach, Phys. Chem. Chem. Phys. **19**, 3544 (2017).
[68]J. Binns, K. V. Kamenev, K. E. R. Marriott, G. J. McIntyre, S. A. Moggach, M. Murrie, and S. Parsons, Chem. Commun. **52**, 7486 (2016).
[69]Q. Zeng, K. Wang, Y. Qiao, X. Li, and B. Zou, J. Phys. Chem. Lett. **8**, 1436 (2017).
[70]W. Cai, A. Gładysiak, M. Anioła, V. J. Smith, L. J. Barbour, and A. Katrusiak, J. Am. Chem. Soc. **137**, 9296 (2015).
[71]S. A. Hodgson, J. Adamson, S. J. Hunt, M. J. Cliffe, A. B. Cairns, A. L. Thompson, M. G. Tucker, N. P. Funnell, and A. L. Goodwin, Chem. Commun. **50**, 5264 (2014).
[72]G. N. Greaves, A. L. Greer, R. S. Lakes, and T. Rouxel, Nat. Mater. **10**, 823 (2011).
[73]I. Beurroies, M. Boulhout, P. L. Llewellyn, B. Kuchta, G. Férey, C. Serre, and R. Denoyel, Angew. Chem. Int. Ed. **49**, 7526 (2010).
[74]A. Ghoufi, A. Subercaze, Q. Ma, P. G. Yot, Y. Ke, I. Puente-Orench, T. Devic, V. Guillerm, C. Zhong, C. Serre, G. Férey, and G. Maurin, J. Phys. Chem. C **116**, 13289 (2012).

[75]J. Rodriguez, I. Beurroies, M.-V. Coulet, P. Fabry, T. Devic, C. Serre, R. Denoyel, and P. L. Llewellyn, Dalton Trans. **45**, 4274 (2016).
[76]S. Henke, M. T. Wharmby, G. Kieslich, I. Hante, A. Schneemann, Y. Wu, D. Daisenberger, and A. K. Cheetham, Chem. Sci. **9**, 1654 (2018).
[77]P. Vervoorts, C. L. Hobday, M. G. Ehrenreich, D. Daisenberger, and G. Kieslich, Z. Anorg. Allg. Chem. **645**, 970 (2019).
[78]A. J. Graham, A.-M. Banu, T. Düren, A. Greenaway, S. C. McKellar, J. P. S. Mowat, K. Ward, P. A. Wright, and S. A. Moggach, J. Am. Chem. Soc. **136**, 8606 (2014).
[79]R. N. Widmer, G. I. Lampronti, N. Casati, S. Farsang, T. D. Bennett, and S. A. Redfern, Phys. Chem. Chem. Phys. **21**, 12389 (2019).
[80]I. E. Collings, M. Bykov, E. Bykova, M. Hanfland, S. van Smaalen, L. Dubrovinsky, and N. Dubrovinskaia, CrystEngComm **20**, 3512 (2018).
[81]I. E. Collings, R. S. Manna, A. A. Tsirlin, M. Bykov, E. Bykova, M. Hanfland, P. Gegenwart, S. van Smaalen, L. Dubrovinsky, and N. Dubrovinskaia, Phys. Chem. Chem. Phys. **20**, 24465 (2018).
[82]M. Ptak, I. E. Collings, K. L. Svane, A. Sieradzki, W. Paraguassu, and M. Mączka, J. Mater. Chem. C **7**, 8660 (2019).
[83]M. Mączka, I. E. Collings, F. F. Leite, and W. Paraguassu, Dalton Trans. **48**, 9072 (2019).
[84]H. A. Evans, Z. Deng, I. E. Collings, Y. Wu, J. L. Andrews, K. Pilar, J. M. Tuffnell, G. Wu, J. Wang, S. E. Dutton, P. D. Bristowe, R. Seshadri, and A. K. Cheetham, Chem. Commun. **55**, 2964 (2019).
[85]I. E. Collings, A. B. Cairns, A. L. Thompson, J. E. Parker, C. C. Tang, M. G. Tucker, J. Catafesta, C. Levelut, J. Haines, V. Dmitriev, P. Pattison, and A. L. Goodwin, J. Am. Chem. Soc. **135**, 7610 (2013).
[86]S. H. Lapidus, G. J. Halder, P. J. Chupas, and K. W. Chapman, J. Am. Chem. Soc. **135**, 7621 (2013).
[87]J. A. Gould, M. J. Rosseinsky, J. E. Warren, and S. Moggach, Z. Kristallogr. **229**, 123 (2014).
[88]I. E. Collings, M. Bykov, E. Bykova, M. G. Tucker, S. Petitgirard, M. Hanfland, K. Glazyrin, S. van Smaalen, A. L. Goodwin, L. Dubrovinsky, and N. Dubrovinskaia, CrystEngComm **18**, 8849 (2016).
[89]M. Mączka, P. Kadłubański, P. T. C. Freire, B. Macalik, W. Paraguassu, K. Hermanowicz, and J. Hanuza, Inorg. Chem. **53**, 9615 (2014).
[90]L. Xin, Z. Fan, G. Li, M. Zhang, Y. Han, J. Wang, K. P. Ong, L. Qin, Y. Zheng, and X. Lou, New J. Chem. **41**, 151 (2017).
[91]M. Mączka, T. A. da Silva, W. Paraguassu, and K. P. da Silva, Spectrochim. Acta A **156**, 112 (2016).
[92]M. Ptak, K. L. Svane, A. Walsh, and W. Paraguassu, Phys. Chem. Chem. Phys. **21**, 4200 (2019).
[93]M. Andrzejewski and A. Katrusiak, J. Phys. Chem. Lett. **8**, 279 (2017).
[94]E. C. Spencer, M. S. Kiran, W. Li, U. Ramamurty, N. L. Ross, and A. K. Cheetham, Angew. Chem. Int. Ed. **53**, 5583 (2014).
[95]S. S. Bhat, W. Li, A. K. Cheetham, U. V. Waghmare, and U. Ramamurty, Phys. Chem. Chem. Phys. **18**, 19032 (2016).
[96]M. Andrzejewski and A. Katrusiak, J. Phys. Chem. Lett. **8**, 929 (2017).
[97]A. Półrolniczak, S. Sobczak, and A. Katrusiak, Inorg. Chem. **57**, 8942 (2018).
[98]A. Lanza, L. S. Germann, M. Fisch, N. Casati, and P. Macchi, J. Am. Chem. Soc. **137**, 13072 (2015).
[99]E. C. Spencer, R. J. Angel, N. L. Ross, B. E. Hanson, and J. A. K. Howard, J. Am. Chem. Soc. **131**, 4022 (2009).
[100]J. K. Clegg, A. J. Brock, K. A. Jolliffe, L. F. Lindoy, S. Parsons, P. A. Tasker, and F. J. White, Chem. Eur. J. **23**, 12480 (2017).
[101]Z. Yang, G. Cai, C. L. Bull, M. G. Tucker, M. T. Dove, A. Friedrich, and A. E. Phillips, Philos. Trans. R. Soc. A **377**, 20180227 (2019).
[102]M. Viswanathan, CrystEngComm **20**, 6861 (2018).
[103]D. A. Keen, A. L. Goodwin, M. G. Tucker, M. T. Dove, J. S. O. Evans, W. A. Crichton, and M. Brunelli, Phys. Rev. Lett. **98**, 225501 (2007).
[104]L. H. N. Rimmer, M. T. Dove, A. L. Goodwin, and D. C. Palmer, Phys. Chem. Chem. Phys. **16**, 21144 (2014).
[105]K. W. Chapman, G. J. Halder, and P. J. Chupas, J. Am. Chem. Soc. **131**, 17546 (2009).
[106]I. Peral and J. Íñiguez, Phys. Rev. Lett. **97**, 225502 (2006).
[107]T. D. Bennett, P. Simoncic, S. A. Moggach, F. Gozzo, P. Macchi, D. A. Keen, J.-C. Tan, and A. K. Cheetham, Chem. Commun. **47**, 7983 (2011).
[108]R. N. Widmer, G. I. Lampronti, S. Anzellini, R. Gaillac, S. Farsang, C. Zhou, A. M. Belenguer, H. Palmer, A. K. Kleppe, M. T. Wharmby, S. A. T. Redfern, F.-X. Coudert, S. G. MacLeod, and T. D. Bennett, Nat. Mater. **18**, 370 (2019).
[109]S. Cao, T. D. Bennett, D. A. Keen, A. L. Goodwin, and A. K. Cheetham, Chem. Commun. **48**, 7805 (2012).
[110]T. D. Bennett, A. L. Goodwin, M. T. Dove, D. A. Keen, M. G. Tucker, E. R. Barney, A. K. Soper, E. G. Bithell, J.-C. Tan, and A. K. Cheetham, Phys. Rev. Lett. **104**, 115503 (2010).
[111]C. L. Hobday, R. J. Marshall, C. F. Murphie, J. Sotelo, T. Richards, D. R. Allan, T. Düren, F.-X. Coudert, R. S. Forgan, C. A. Morrison, S. A. Moggach, and T. D. Bennett, Angew. Chem. Int. Ed. **55**, 2401 (2016).
[112]C. S. Coates, M. R. Ryder, J. A. Hill, J.-C. Tan, and A. L. Goodwin, APL Mater. **5**, 066107 (2017).
[113]S. A. Moggach, T. D. Bennett, and A. K. Cheetham, Angew. Chem. Int. Ed. **48**, 7087 (2009).
[114]S. Krause, V. Bon, I. Senkovska, U. Stoeck, D. Wallacher, D. M. Többens, S. Zander, R. S. Pillai, G. Maurin, F.-X. Coudert, and S. Kaskel, Nature **532**, 348 (2016).
[115]K. W. Chapman, G. J. Halder, and P. J. Chupas, J. Am. Chem. Soc. **130**, 10524 (2008).
[116]A. J. Graham, D. R. Allan, A. Muszkiewicz, C. A. Morrison, and S. A. Moggach, Angew. Chem. Int. Ed. **50**, 11138 (2011).
[117]I. E. Collings, E. Bykova, M. Bykov, S. Petitgirard, M. Hanfland, D. Paliwoda, L. Dubrovinsky, and N. Dubrovinskaia, Chemphyschem **17**, 3369 (2016).
[118]J. Sotelo, C. H. Woodall, D. R. Allan, E. Gregoryanz, R. T. Howie, K. V. Kamenev, M. R. Probert, P. A. Wright, and S. A. Moggach, Angew. Chem. Int. Ed. **54**, 13332 (2015).
[119]S. Jiang, Y. Hu, S. Chen, Y. Huang, and Y. Song, Chem. Eur. J. **24**, 19280 (2018).
[120]C. L. Hobday, C. H. Woodall, M. J. Lennox, M. Frost, K. Kamenev, T. Düren, C. A. Morrison, and S. A. Moggach, Nat. Commun. **9**, 1429 (2018).
[121]S. C. McKellar, J. Sotelo, A. Greenaway, J. P. S. Mowat, O. Kvam, C. A. Morrison, P. A. Wright, and S. A. Moggach, Chem. Mater. **28**, 466 (2016).
[122]J. Im, D. Seoung, G. C. Hwang, J. W. Jun, S. H. Jhung, C.-C. Kao, T. Vogt, and Y. Lee, Chem. Mater. **28**, 5336 (2016).
[123]S. C. McKellar, A. J. Graham, D. R. Allan, M. I. H. Mohideen, R. E. Morris, and S. A. Moggach, Nanoscale **6**, 4163 (2014).
[124]S. Sobczak and A. Katrusiak, Cryst. Growth Des. **18**, 1082 (2018).
[125]Q. Li, S. Li, K. Wang, J. Liu, K. Yang, B. Liu, G. Zou, and B. Zou, J. Phys. Chem. C **118**, 5848 (2014).
[126]M. Andrzejewski, N. Casati, and A. Katrusiak, Dalton Trans. **46**, 14795 (2017).
[127]E. C. Spencer, J. Zhao, N. L. Ross, M. B. Andrews, R. G. Surbella, and C. L. Cahill, J. Solid State Chem. **202**, 99 (2013).
[128]G. Mehlana and S. A. Bourne, CrystEngComm **19**, 4238 (2017).
[129]G. J. Halder, K. W. Chapman, J. A. Schlueter, and J. L. Manson, Angew. Chem. Int. Ed. **50**, 419 (2011).
[130]B. Wehinger, C. Fiolka, A. Lanza, R. Scatena, M. Kubus, A. Grockowiak, W. A. Coniglio, D. Graf, M. Skoulatos, J.-H. Chen, J. Gukelberger, N. Casati, O. Zaharko, P. Macchi, K. W. Krämer, S. Tozer, C. Mudry, B. Normand, and C. Rüegg, Phys. Rev. Lett. **121**, 117201 (2018).
[131]W. Kaneko, M. Mito, S. Kitagawa, and M. Ohba, Chemistry **14**, 3481 (2008).
[132]P. Quintero, D. Rajan, M. Peprah, T. Brinzari, R. S. Fishman, D. R. Talham, and M. W. Meisel, Phys. Rev. B **91**, 014439 (2015).
[133]A. C. McConnell, J. D. Bell, and J. S. Miller, Inorg. Chem. **51**, 9978 (2012).
[134]G. Handzlik, B. Sieklucka, H. Tomkowiak, A. Katrusiak, and D. Pinkowicz, Magnetochemistry **5**, 33 (2019).
[135]M. Ohba, W. Kaneko, S. Kitagawa, T. Maeda, and M. Mito, J. Am. Chem. Soc. **130**, 4475 (2008).
[136]G. Levchenko, A. B. Gaspar, G. Bukin, L. Berezhnaya, and J. A. Real, Inorg. Chem. **57**, 8458 (2018).

[137]A. B. Gaspar, G. Levchenko, S. Terekhov, G. Bukin, J. Valverde-Muñoz, F. J. Muñoz Lara, M. Seredyuk, and J. A. Real, Eur. J. Inorg. Chem. **2014**, 429.
[138]N. F. Sciortino, F. Ragon, K. A. Zenere, P. D. Southon, G. J. Halder, K. W. Chapman, L. Piñeiro-López, J. A. Real, C. J. Kepert, and S. M. Neville, Inorg. Chem. **55**, 10490 (2016).
[139]G. Levchenko, G. V. Bukin, S. A. Terekhov, A. B. Gaspar, V. Martínez, M. C. Muñoz, and J. A. Real, J. Phys. Chem. B **115**, 8176 (2011).
[140]J. Yang, L. Zhou, J. Cheng, Z. Hu, C. Kuo, C.-W. Pao, L. Jang, J.-F. Lee, J. Dai, S. Zhang, S. Feng, P. Kong, Z. Yuan, J. Yuan, Y. Uwatoko, T. Liu, C. Jin, and Y. Long, Inorg. Chem. **54**, 6433 (2015).
[141]J. M. Bermúdez-García, M. Sánchez-Andújar, S. Castro-García, J. López-Beceiro, R. Artiaga, and M. A. Señarís Rodríguez, Nat. Commun. **8**, 15715 (2017).
[142]T. D. Bennett and A. K. Cheetham, Acc. Chem. Res. **47**, 1555 (2014).
[143]A. M. Arevalo-Lopez, B. Liang, M. S. Senn, C. Murray, C. Tang, and J. P. Attfield, J. Mater. Chem. C **2**, 9364 (2014).
[144]S. S. Lobanov, J. A. Daly, A. F. Goncharov, X. Chan, S. K. Ghose, H. Zhong, L. Ehm, T. Kim, and J. B. Parise, J. Phys. Chem. A **122**, 6109 (2018).
[145]N. A. Benedek and C. J. Fennie, Phys. Rev. Lett. **106**, 107204 (2011).
[146]H. L. B. Boström, M. S. Senn, and A. L. Goodwin, Nat. Commun. **9**, 2380 (2018).
[147]F.-X. Coudert, Acta Crystallogr. B **71**, 585 (2015).
[148]P. G. Yot, L. Vanduyfhuys, E. Alvarez, J. Rodriguez, J.-P. Itié, P. Fabry, N. Guillou, T. Devic, I. Beurroies, P. L. Llewellyn, B. Van Speybroeck, C. Serre, and G. Maurin, Chem. Sci. **7**, 446 (2016).
[149]Z. Su, Y.-R. Miao, G. Zhang, J. T. Miller, and K. S. Suslick, Chem. Sci. **8**, 8004 (2017).
[150]X. Zhou, Y.-R. Miao, W. L. Shaw, K. S. Suslick, and D. D. Dlott, J. Am. Chem. Soc. **141**, 2220 (2019).
[151]W. Zhou, H. Wu, T. Yildirim, J. R. Simpson, and A. R. Hight Walker, Phys. Rev. B **78**, 054114 (2008).
[152]Y. Wu, A. Kobayashi, G. J. Halder, V. K. Peterson, K. W. Chapman, N. Lock, P. D. Southon, and C. J. Kepert, Angew. Chem. **120**, 9061 (2008).
[153]C. S. Coates and A. L. Goodwin, Mater. Horiz. **6**, 211 (2019).
[154]R. Mittal, S. L. Chaplot, H. Schober, and T. A. Mary, Phys. Rev. Lett. **86**, 4692 (2001).